

Journal of Materials Chemistry C

Accepted Manuscript



This is an *Accepted Manuscript*, which has been through the Royal Society of Chemistry peer review process and has been accepted for publication.

Accepted Manuscripts are published online shortly after acceptance, before technical editing, formatting and proof reading. Using this free service, authors can make their results available to the community, in citable form, before we publish the edited article. We will replace this *Accepted Manuscript* with the edited and formatted *Advance Article* as soon as it is available.

You can find more information about *Accepted Manuscripts* in the [Information for Authors](#).

Please note that technical editing may introduce minor changes to the text and/or graphics, which may alter content. The journal's standard [Terms & Conditions](#) and the [Ethical guidelines](#) still apply. In no event shall the Royal Society of Chemistry be held responsible for any errors or omissions in this *Accepted Manuscript* or any consequences arising from the use of any information it contains.

Cite this: DOI: 10.1039/c0xx00000x

www.rsc.org/xxxxxx

ARTICLE TYPE

A facile synthesis of phase-pure FeCr₂Se₄ and FeCr₂S₄ nanocrystals via a wet chemistry method

Xiang Mao, Jaebeom Lee*

Received (in XXX, XXX) XthXXXXXXXXXX 20XX, Accepted Xth XXXXXXXXXXXX 20XX

DOI: 10.1039/b000000x

We report a novel facile route for synthesis of iron-based ternary nanocrystals (NCs), i.e., FeCr₂Se₄ and FeCr₂S₄, using a wet chemistry method. The electronic structure with a narrow band gap of Fe-based ternary semiconducting NCs with different dopants it offers promising conductive properties. Owing significantly to the non-toxicity of their constituent materials, they exhibit higher potential for being utilized in solar cells than Cd and Pb-based compounds. The general route of synthesis for ternary compounds includes mixing and reacting of different elemental powders in evacuated silica ampoules for long periods of time under high temperature (700–1000 °C). However, this process results in uncontrolled size and morphology of the colloidal NCs. In our proposed method, the NC morphology was easily controlled by the solvent and heating temperature, multi-utilizing oleylamine as surfactant, solvent, and reducing agent. The synthesized NCs possess excellent mono-dispersity of size and shape without any aggregation and the conductivities of the deposited layer of FeCr₂Se₄ and FeCr₂S₄ NCs were 3.25 μA and 2.33 μA, respectively. Therefore, these iron-based NCs may replace the use of chalcogenides those are known to be environmentally toxic, and may contribute to low efficiency of energy transfer.

Introduction

Metal chalcogenide materials have gained significant attention because of their interesting coordination, semiconducting behavior, and large binding affinity for metal ions.^{1,2} Their applications range from bio-labeling to photocatalysis and photovoltaics that utilize either the discrete or collective properties of these size-controlled nanocrystals (NCs).³ The synthesis of the archetypal binary (II–VI) NCs has progressed to where precise control over their size, shape, composition, and crystal phase has been achieved.^{4,5} The extension of the colloidal NC synthesis method to ternary and quaternary semiconductors or other functional materials has great potential.^{6–12} Metal-based ternary NCs such as MCr₂X₄ (where M = Cd, Zn, Hg and Co; X = S, Se, and Te) have been considered as functional materials and their structural analysis has been carried out.¹³ The advancement in the colloidal synthesis and shape control of these bimetallic, ternary, and quaternary NCs has been demonstrated well enough, although copper composites remain elusive.^{14–16}

Iron-based metallic NCs are mainly synthesized with the polyphase forms of FeSe, FeSe₂, FeCr₂S₄, FeCr₂Se₄, and Fe_{0.5}Cu_{0.5}Cr₂Se₄ and so on. These NCs are of interest because of abundant Fe and Cr resources, their unique superconducting and optical properties, and appropriate optical energy band gaps for solar cell application.^{17–20} The synthesis and utilization of these materials are growing fields of research.^{20,21} However, only a few studies have been reported on the synthesis of iron-based ternary materials using wet chemical synthesis methods.^{21,22}

The Goldschmidt-Penn-Parrott law for crystal conductivity

depicts $\Delta W/W \propto L_s^{1/2}$, where ΔW is the increase in crystal resistivity W and L_s indicates the average grain size.²³ This implies that the grain size of the crystals is an essential factor to consider. Concurrently, crystal group contribution (λ_L) also influences the natural conductivity of the crystals: $\lambda_L = L\sigma T$, where L is the Lorentz factor, σ indicates the extent of the crystallization of the NCs and T is the temperature used for conductivity measurements. From these two equations, it can be concluded that for higher conductivity, smaller size and higher crystallinity are required.^{24–26} Additionally, iron-based ternary NCs (FeCr₂Se₄ and FeCr₂S₄ NCs) are attractive for their electrical applications since the conductivity can be influenced by external temperature and lattice contribution of the NCs as well as by the different dopants during synthesis.²⁷

Recently, some studies have shown synthesis of FeCr₂Se₄ and FeCr₂S₄ NCs that involve the use of powder precursors, hot-pressing, high-temperature (700–1000 °C), and additives leading to significant increases in the conductivity of the microscale products; however the synthesis is disadvantaged because of the scarcity and high cost of the metal precursors. Extensive efforts have been undertaken to develop highly conductive, durable, and low-cost alternative methods such as metal transitional element of diffusion²⁸ and high-temperature sealed methods.^{29,30} However, most non-precious metal conductors suffer from poor conductivity. In addition, the facile synthesis of iron-based ternary metal chalcogenides with morphology control was not found to be practicable via wet chemistry methods.

Herein, we describe a novel wet chemistry method to synthesize colloidal crystals of mono-dispersed and phase-pure

stoichiometric FeCr_2Se_4 and $\text{FeCr}_2\text{S}_4\text{NCs}$ with high yield. The synthesis method reported in this study is advantageous as it utilizes less energy, takes place under atmospheric pressure, and employs standard chemicals (Fe/Cr/Se/S composition, purity 98%). Moreover, the morphology control of the NCs was realized by the simple presence of a primary amine of alkene i.e., oleylamine (OLA), due to solvent coordination and its passivation to the NC surface,^{16b} which suggests that OLA can not only be used as the solution medium, but also as the stabilizer on the surface of the NCs in the passivation process. The reaction finished completely within 30min. The anisotropic growth mechanism for NCs in a solid solution has been investigated in detail by controlling their growth kinetics, where the reaction temperature is an essential factor. At 330–360°C, the formation of the NCs was predominantly favored, whereas below this range, only the precursors such as Cr_2S_3 , Cr_3S_4 , FeS, FeSe, or FeSe_2 were fabricated.^{13c,31} Moreover, the electrical properties of the multi-layered NCs on a glass substrate with gold electrodes was demonstrated, offering the possibility of an optimum crystal structure via this synthesis method for efficient conductive devices. The magnetic properties of the NCs were also characterized.

Experimental details

Chemicals

Iron(II) acetylacetonate($\text{Fe}(\text{acac})_2$, 99.8%), chromium (III) acetylacetonate ($\text{Cr}(\text{acac})_3$, 99.8%), anhydrous acetonitrile (>95%), 1,2-ethanedithiol (EDT, 95%), selenium powder (100 mesh, 98%), oleylamine (OLA, 98%), 1-dodecanethiol (1-DDT, 98%), toluene (99%), chloroform (99%), isopropanol(90%), ethanol (90%) were used. All of these chemicals were purchased from Sigma-Aldrich.

Selenium precursor preparation

10-mL of OLA and 0.03-mol of Se powder were mixed in a flask, and vacuum-pumped at 120 °C for 30min. Subsequently, the flask was purged with N_2 during the reaction to prevent any unwanted oxidation. This solution was heated at 330 °C for over 1 h, and maintained at that temperature for an hour. When the Se powder completely dissolved in OLA, the color of the solution changed from colorless to maroon, finally attaining a faint yellow hue.

Synthesis of FeCr_2Se_4 NCs

FeCr_2Se_4 NCs were synthesized under N_2 without any water and in the presence of oxygen using standard Schlenk techniques. A typical synthesis of FeCr_2Se_4 NCs is detailed as follows; first, 0.025-mmol $\text{Fe}(\text{acac})_2$, 0.50-mmol $\text{Cr}(\text{acac})_3$ and 10-ml OLA were mixed at room temperature, where the molar ratio of Fe:Cr was carefully investigated to optimize for a homogeneous product(see Fig. S5 further details). The mixed solution was cycled between vacuum and N_2 three times. Afterwards, the mixture was kept at 60 °C under vacuum for 1h, and then heated to 120 °C under vigorous stirring. 10min later, the mixture was heated directly to 335°C. Once the temperature reached 335°C, 1mL of the prepared Se precursor was dropped into the mixture at an injection rate of 3 drops sec^{-1} using a 10mL injection syringe under vigorous stirring. The temperature was kept at

335°C for another 30min after completion of the injection. Then, the flask was cooled to room temperature to produce the NCs.

The synthesized NCs were purified by precipitation with isopropanol via centrifugation at 8,500rpm for 20min, and re-dispersed in toluene or chloroform. After repetition of 3–4 times of the washing step, the supernatant containing unreacted precursors and by-products was discarded completely. The final product was either dried as a powder sample in vacuum or dissolved in toluene or chloroform to form a stable sample solution.

Synthesis of FeCr_2S_4 NCs

The method for synthesis of FeCr_2S_4 NCs was similar to the previously described method except that the Se precursor was replaced by 1-DDT. 0.15-mmol (0.1-mL) of 1-DDT was injected into the mixture rapidly under vigorous stirring. The temperature was kept constant at 335°C for 30min. Then, the flask was cooled to room temperature. The purified process was as described previously. The final $\text{FeCr}_2\text{S}_4\text{NCs}$ were re-dispersed in toluene or chloroform to form a stable sample solution.

Device fabrication and characterization

A conductivity response device was fabricated (Fig. 5). Au film with thickness of 100nm was constructed by radio frequency magnetron after a standard photolithography process. The middle section of the Au film was removed in order to deposit the concentrated colloidal NC solution through spin-coating, and then the prepared device was kept dry under vacuum condition. The dried film was immersed in 0.2-molL⁻¹ EDT solution in anhydrous acetonitrile for 1h and then dried by stable N_2 gas blowing. This process was repeated to increase layer thickness, whereby any redundant organisms were removed by EDT treatment.

Electron imaging and element analysis were carried out using high resolution transmission electron microscopy(HRTEM, Hitach-7600, Japan) at an acceleration voltage of 200KV with a CCD camera (1350×1040), scanning electron microscopy (SEM, Hitachi-S4700, Japan) and energy dispersive X-ray spectroscopy (EDX). XRD analysis was carried out using an X-ray diffractometer (Empyrean series-2, Netherlands). Optical spectra were obtained using a UV-Vis spectrophotometer (Scinco S310, Korea) and FT-IR spectroscopy (Jasco 6300, Japan). Thermal gravimetric analysis (TGA, Scinco N-1000, Korea) was carried out under N_2 atmosphere at a heating rate of 15 °C/min from room temperature to 800°C. I-V characteristics were recorded using Iviumstat Electrochemical Interface (Two-point method, Netherlands). The magnetic properties of each NC was characterized by superconducting quantum interference device (MPMS5, USA with sensitivity of 10⁻⁸emu, field range of -7 T–+7 T, and temperature range of 1.7 K–400 K).

Results and discussion

TEM images showed that the FeCr_2Se_4 NCs were formed with a predominantly quadrilateral shape a tan average size of 63.4±1.7-nm(Fig. 1A, B and insert). In the HRTEM micrograph of an individual NC, the lattice fringes were distinct and the NCs showed good crystallization with a *d*-spacing of 0.3315-nm,

corresponding to the (201) reflection of monoclinic FeCr_2Se_4 NCs (Fig. 1C). The TEM images of the other NCs also indicated excellent morphology and high crystallinity (see Fig. S1). The angles between the planes, as measured from the selected area electron diffraction (SAED) obtained from Fig. 1D, was consistent with the expected value for these two planes in a crystal lattice. The iron-based ternary sulfur NCs (FeCr_2S_4) were composed of mostly spherical particles (Fig. 2). The average size of the individual particles along the (220) direction of the NCs was 13.6 ± 0.6 nm. The d -spacing was 0.3531 nm, corresponding to the (220) planes of the daubreelite phase FeCr_2S_4 NCs.

Fig. S2 shows a dramatic morphology transformation of the respective NCs during the growth process. The average elemental composition of the samples was determined using EDX, resulting in a Fe/Cr/Se ratio of 1:1.67:3.87 for FeCr_2Se_4 , and a Fe/Cr/S ratio of 1:2.13:3.64 for FeCr_2S_4 NCs (see Figs. S3 and S4). Fig. S5 presents typical TEM images of the final products prepared by simple control of the molar ratios of the Fe, Cr, Se, S precursors used in various ways during the same synthesis process. It is observed that crystal morphology or size distribution of the NCs is quite different although nanostructures were obtained in all cases. We are at present investigating the influence of precursors' molar ratio in the OLA on the morphology and size of the NCs.

Fig. 3A presents powder X-ray diffraction (PXRD) patterns corresponding to the monoclinic and daubreelite phases of FeCr_2Se_4 and FeCr_2S_4 , respectively. The major diffraction peaks were indexed as (201), (002), (310), (311), (003), and (313) reflections of FeCr_2Se_4 (ICCD no. 65-4103). Similar statistics demonstrated the diffraction and reflections of FeCr_2S_4 NCs (ICCD no. 65-8993). In both cases the peaks correspond well with previously reported standard XRD patterns. In our novel crystal synthesis, OLA played multiple roles (i.e., surfactant, solvent, and reducing agent) as it possesses a special molecular chain such as the double bond between the 9th and 10th carbon atoms. Restriction of rotation at the position of the double bond perhaps enables the elemental grains to attach together, thus reducing the surface energy.^{13c} Therefore, NCs were passivated well and protected by the OLA in our experiment.

This assumption of surface modification was confirmed by the FT-IR analysis of the characteristic peaks of OLA in the NCs (Fig. 3B). The absence of distinct IR peaks for -SH group (2520cm^{-1}) indicated that 1-DDT was not included in the final purified FeCr_2S_4 NCs; i.e., the sulfur precursor was completely consumed in the reaction mixture. Moreover, the appearance of IR peaks for NH_2 groups (2975-cm^{-1}) can be explained by the formation of covalent bonds between the NH_2 group and the surface of each NC.

For the FeCr_2Se_4 and FeCr_2S_4 NCs, the color of the colloidal solution was brown-yellow and light-black, respectively. Absorption spectroscopy was subsequently performed to study the band gaps of these NCs. As shown in Fig. 4A, the onset absorption begins near 870 nm for FeCr_2Se_4 NCs and 854 nm for FeCr_2S_4 NCs. By calculating the band gaps of the NCs with the Kubelka-Munk method, the indirect bandgaps of FeCr_2Se_4 NCs and FeCr_2S_4 NCs are determined to be 0.88 and 0.91 eV, respectively, and the direct bandgaps are 2.36 eV for FeCr_2Se_4 NCs and 2.67 eV for FeCr_2S_4 NCs (Fig. 4B-D). These indirect band gaps are probably due to the size effect of the as-synthesized NCs

or the change of crystallographic structure of the NCs.^{32b}

The magnetizations of the two samples were measured as functions of external magnetic field to evaluate the saturation magnetization at 5K and 300K (see Fig. S7). The highest magnetization values obtained at 5K for FeCr_2Se_4 and FeCr_2S_4 NCs are of similar value of 0.2-emug^{-1} . Both NCs exhibit magnetic behavior near room temperature whereas antiferromagnetic behavior with relatively low coercivity values of ca. $5 \times 10^3\text{Oe}$ (FeCr_2Se_4) and ca. $1 \times 10^4\text{Oe}$ (FeCr_2S_4) was observed at 5K. The variation in magnetization as a function of temperature under field-cooled (FC) and zero-field-cooled (ZFC) conditions with an applied magnetic field of 500e was analyzed. The observed blocking temperature (T_b) from low-field 500e measurements for FeCr_2Se_4 and FeCr_2S_4 NCs were 180K and 176K, respectively. The measurements showed a drop in the magnetization value to nearly zero at a temperature between 220K and 230K for both samples (see Fig. S8). This can be ascribed to their Curie temperatures (T_c), which were somewhat higher than the bulk value of 180K due to the orbital ordering transition at low temperatures due to a static cooperative Jahn-Teller effect.^{29;32}

Fig. 5 shows I-V curves that indicate the conductivity of FeCr_2Se_4 and FeCr_2S_4 NCs in the devices. The SEM images of the device fabrication are presented in Fig. S9. The current values from the films were obtained by adjusting the voltage from +4 V to -4 V, and the current values obtained were $-3.25\mu\text{A}$ to $+3.25\mu\text{A}$ (FeCr_2Se_4) and $-2.33\mu\text{A}$ to $+2.33\mu\text{A}$ (FeCr_2S_4), respectively. Furthermore, the two-point I-V plots showed a turn-on potential varying between -1.25 to +1.25 eV in the negative and positive quadrants, respectively (see Fig. S10). Compared with similar experimental studies, the current value of these two kinds of NCs is similar to the values obtained from copper-based ternary or quaternary NCs employed in solar cell applications with $0.024\mu\text{A}$ or $1.5\mu\text{A}$.^{33;34} These iron-based ternary NCs are thus promising compounds as they are semiconducting and can be easily doped by substituting different chalcogens.³⁵ Additionally, the conductivity is usually dominated by photon or lattice conductivity, and the unit cell showed the ternary structures as monoclinic and daubreelite phases respectively.^{36;37} It is natural that crystalline size and lattice contribution affect internal structural distortions of the NC, resulting in the final conductivity. Among these two kinds of coordination structure in the NCs, Cr^{3+} has three electrons to fill the majority spin T_{2g} orbital (subsequent band) completely. Thus, Cr^{3+} may provide the metallic carriers. Furthermore, Fe^{2+} provides orbital electrons thus filling the orbital completely. So, these two kinds of NCs (FeCr_2Se_4 and FeCr_2S_4 NCs) can be considered as metal-like materials with high conductivity. Therefore, the conductive film maybe used as an efficient substrate in solar cell construction.

Conclusions

In summary, we have demonstrated a novel wet chemical synthesis method for iron-based ternary FeCr_2Se_4 and FeCr_2S_4 NCs. The method involved the hot injection of S and Se precursors into a boiling coordinating solvent containing the metal ions and surfactant molecules. The specific chemical compositions of these NCs combined with their precursors and

initial electrical response show great potential for future electronic applications.

Acknowledgement

This research was supported by the Basic Science Research Program of the National Research Foundation of Korea (NRF) funded by the Ministry of Education (2013R1A1A4A010004637); and by the Civil & Military Technology Cooperation Program of the National Research Foundation of Korea (NRF) funded by the Ministry of Science, ICT & Future Planning (No. 2013M3C1A9055407).

Notes and references

Department of Nano Fusion Engineering, and Cogno-Mechatronics Engineering, Pusan National University, Busan, 609-735 Republic of Korea

E-mail: jaebeom@pusan.ac.kr

† Electronic Supplementary Information (ESI) available: [The detailed experimental procedures, additional TEM images, SEM, EDX, TGA, I-V curves, SQUID curves, and the image of fabrication devices are given in the Supporting Information.]. See DOI: 10.1039/b000000x/

- (a) P. Feng, X. Bu, and N. Zheng, *Accounts Of Chemical Research*, 2005, **38**, 293; (b) I. Chung, J. I. Jang, C. D. Malliakas, J. B. Ketterson, and M. G. Kanatzidis, *Journal of the American Chemical Society*, 2009, **132**, 384
- (a) W. S. Sheldrick and M. Wachhold, *Angewandte Chemie International Edition*, 1997, **36**, 206; (b) M. Y. C. Teo, S. A. Kulinich, O. A. Plaksin, and A. L. Zhu, *The Journal of Physical Chemistry A*, 2010, **114**, 4173; (c) J. K. Sahoo, M. N. Tahir, A. Yella, T. D. Schladt, S. Pfeiffer, B. Nakhjavan, E. Mugnaioli, U. Kolb, and W. Tremel, *Chemistry of Materials*, 2011, **23**, 3534.
- (a) Buchez, M. Moronne, P. Gin, S. Weiss, and A. P. Alivisatos, *Science*, 1998, **281**, 2013; (b) L. A. Padilha, J. T. Stewart, R. L. Sandberg, W. K. Bae, W. K. Koh, J. M. Pietryga, and V. I. Klimov, *Accounts Of Chemical Research*, 2013, **46**, 1261.
- Z. A. Peng and X. Peng, *Journal of the American Chemical Society*, 2001, **123**, 183.
- K. Ding, Z. Miao, Z. Liu, Z. Zhang, B. Han, G. An, S. Miao, and Y. Xie, *Journal of the American Chemical Society*, 2007, **129**, 6362.
- A. Singh, H. Geaney, F. Laffir, and K. M. Ryan, *Journal of the American Chemical Society*, 2012, **134**, 2910.
- R. B. Soriano, I. U. Arachchige, C. D. Malliakas, J. Wu, and M. G. Kanatzidis, *Journal of the American Chemical Society* 2012, **135**, 768.
- M. E. Norako and R. L. Brutchey, *Chemistry of Materials*, 2010, **22**, 1613.
- I. U. Arachchige, J. Wu, V. P. Dravid, and M. G. Kanatzidis, *Advanced Materials*, 2008, **20**, 3638.
- M. Ibáñez, R. Zamani, W. Li, A. Shavel, J. Arbiol, J. R. Morante, and A. Cabot, *Crystal Growth & Design*, 2012, **12**, 1085.
- C. Zou, L. Zhang, D. Lin, Y. Yang, Q. Li, X. Xu, X. Chen, and S. Huang, *CrystEngComm*, 2011, **13**, 3310.
- J. van Embden, K. Latham, N. W. Duffy, and Y. Tachibana, *Journal of the American Chemical Society*, 2013, **135**, 11562.
- (a) J. Zwinscher and H. D. Lutz, *Journal of Solid State Chemistry*, 1995, **118**, 43; (b) Y. H. Wang, N. Bao, L. Shen, P. Padhan, and A. Gupta, *Journal of the American Chemical Society*, 2007, **129**, 12408; (c) K. Ramasamy, D. Mazumdar, Z. Zhou, Y. H. Wang, and A. Gupta, *Journal of the American Chemical Society*, 2011, **133**, 20716.
- M. E. Norako, M. J. Greaney, and R. L. Brutchey, *Journal of the American Chemical Society*, 2011, **134**, 23.
- X. Lu, Z. Zhuang, Q. Peng, and Y. Li, *CrystEngComm*, 2011, **13**, 4039.
- (a) M. Kruszynska, H. Borchert, J. Parisi, and J. Kolny-Olesiak, *Journal of the American Chemical Society*, 2010, **132**, 15976; (b) Mourdikoudis, S.; Liz-Marzan, L. M. *Chemistry of Materials* 2013, **25**, 1465.
- M. R. Spender and A. H. Morrish, *Canadian Journal of Physics*, 1972, **50**, 1125.
- M. A. Abosedira, *Journal Material Science*, 2008, **8**, 660.
- Y. Mizuguchi, F. Tomioka, S. Tsuda, T. Yamaguchi, and Y. Takano, *Applied Physics Letters*, 2008, **93**, 152505 (03).
- B. Yuan, W. Luan, and S. t. Tu, *Dalton Transactions*, 2012, **41**, 772.
- P. Kumar, S. Uma, and R. Nagarajan, *Chemical Communications*, 2013, **49**, 7316.
- A. M. Wiltrout, N. J. Freymeyer, T. Machani, D. P. Rossi, and K. E. Plass, *Journal of Materials Chemistry*, 2011, **21**, 19286.
- S. Yoshimura, H. Asano, Y. Nakamura, K. Yamaji, Y. Takeda, M. Matsui, S. Ishida, Y. Nozaki, and K. Matsuyama, *Journal of Applied Physics*, 2008, **103**, 7D716.
- Y. Sun and J. A. Rogers, *Advanced Materials*, 2007, **19**, 1897.
- V. Zestrea, V. Y. Kodash, V. Felea, P. Petrenco, D. V. Quach, J. R. Groza, and V. Tsurkan, *Journal of Materials Science*, 2008, **43**, 660.
- H. S. Carslaw and J. C. Jaeger, *Conduction of Heat in Solids*, 1959.
- P. Gibart, M. Robbins, and V. G. Lambrecht Jr, *Journal of Physics and Chemistry of Solids*, 1973, **34**, 1363.
- B. I. Min, S. S. Baik, H. C. Choi, S. K. Kwon, and J. S. Kang, *New Journal of Physics*, 2008, **10**, 055014.
- J. H. Kang, S. J. Kim, B. W. Lee, and C. S. Kim, *Journal of applied physics*, 2006, **99**, 08F714.
- S. J. Kim, B. S. Son, B. W. Lee, and C. S. Kim, *Journal of applied physics*, 2004, **95**, 6837.
- (a) J. Puthussery, S. Seefeld, N. Berry, M. Gibbs, and M. Law, *Journal of the American Chemical Society*, 2010, **133**, 716; (b) J. J. Wang, D. J. Xue, Y. G. Guo, J. S. Hu, and L. J. Wan, *Journal of the American Chemical Society*, 2011, **133**, 18558.
- V. Tsurkan, O. Zaharko, F. Schrettle, C. Kant, J. Deisenhofer, H.-A. K. von Nidda, V. Felea, P. Lemmens, J. R. Groza, and D. V. Quach, *Physical Review B*, 2010, **81**, 184426.
- Y. Liu, D. Yao, L. Shen, H. Zhang, X. Zhang, and B. Yang, *Journal of the American Chemical Society*, 2012, **134**, 7207.
- J. Tang, S. Hinds, S. O. Kelley, and E. H. Sargent, *Chemistry of Materials*, 2008, **20**, 6906.
- T. M. Adams, S. I. bdel-Khalik, S. M. Jeter, and Z. H. Qureshi, *International Journal of Heat and Mass Transfer*, 1998, **41**, 851.
- G. J. Snyder, T. Caillat, and J. P. Fleurial, *Physical Review B*, 2000, **62**, 10185.
- G. Chen, S. G. Volz, T. Borca-Tasciuc, T. Zeng, D. Song, K. L. Wang, and M. S. Dresselhaus, *Thermal Conductivity and Phonon Engineering in Low Dimensional Structures*, 1998.

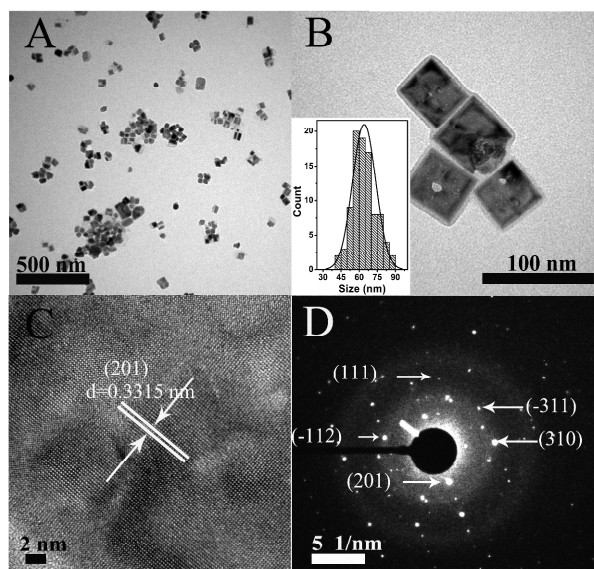


Fig.1(A,B) TEM images of FeCr_2Se_4 NCs, (C) HRTEM images of individual NCs, (D) SAED pattern extracted from image, (inset) size distribution of FeCr_2Se_4 NCs.

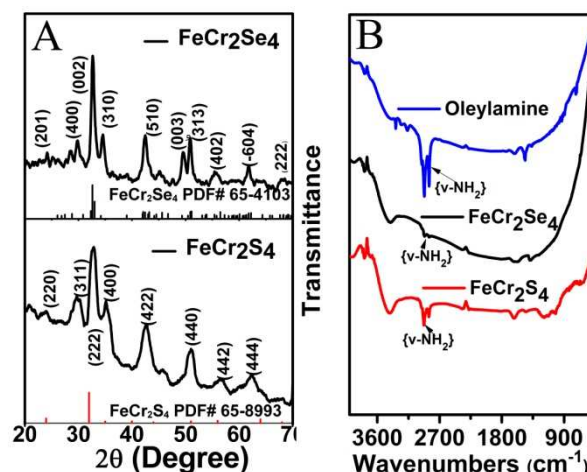


Fig.3(A) PXRD patterns of FeCr_2Se_4 (ICCD no. 65-4103) and FeCr_2S_4 (ICCD no. 65-8993) NCs, standard XRD patterns of parameters are shown at bottom; (B) FT-IR spectra of FeCr_2Se_4 (up), FeCr_2S_4 NCs and oleylamine, respectively.

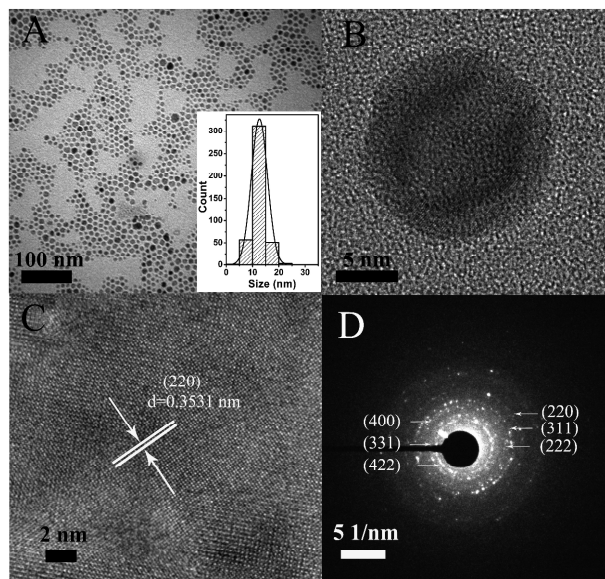


Fig.2(A) TEM images of FeCr_2S_4 NCs, (B,C) HR-TEM images of individual NCs, (D) SAED pattern extracted from image, insets (A) size distribution of FeCr_2S_4 NCs.

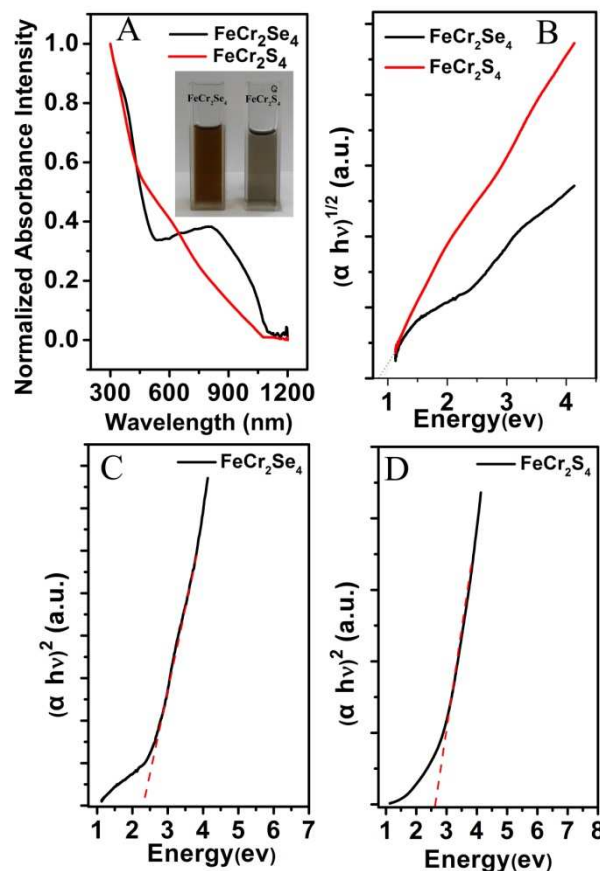


Fig.4 (A) UV-visible absorption spectra of the FeCr_2Se_4 and FeCr_2S_4 NCs, (insert) digital photo of NC solution, left: FeCr_2Se_4 , 6.55-mgL^{-1} ; right: FeCr_2S_4 , 7-mgL^{-1} , (B, C, and D) determination of band gaps by plotting $h\nu^{1/2}$ vs. energy for indirect band gap (B), and $h\nu^2$ vs. energy for direct band gaps (C, D).

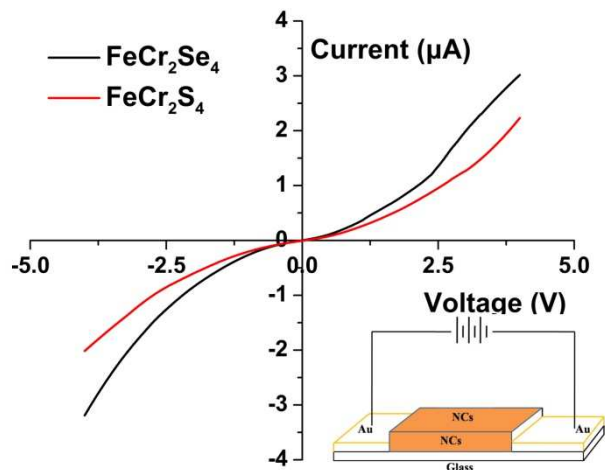
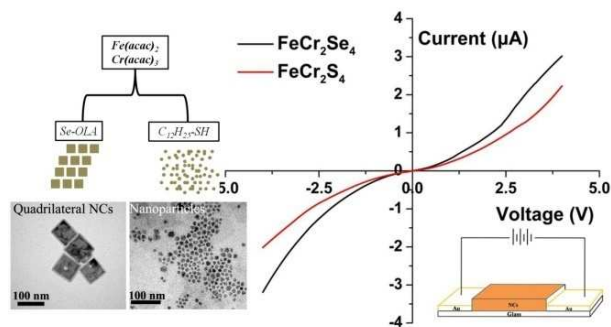


Fig.5 I - V curves of drop-casting films constructed from NCs, black and red lines are current curves of FeCr_2Se_4 and FeCr_2S_4 , respectively. (Insert) configuration for conductivity measurements.

5



TOC Figure Two kinds of Fe-based ternary NCs have been synthesized through injecting different chemical precursors (Se and S) in the wet chemistry method. The NCs have different constructional morphologies, which are of quadrilateral shape (FeCr_2Se_4) and spherical shape (FeCr_2S_4), respectively. Additionally, I - V curves indicate that these two kinds of NCs have comparable conductivity as copper-based NCs used in solar cell applications.

20